

KRITTIKA SUMMER PROJECTS 2021

Kirkwood Gaps

Advait Mehla, Amrit Pucha, Aneesh Bapat, Gaurav Pundir, Harshda Saxena, Muhseen Musthafa, Nihar Apte, Sahil Saha, and Sagar

KRITTIKA SUMMER PROJECTS 2021

Kirkwood Gaps

Advait Mehla^{1,2}, Amrit Pucha³, Aneesh Bapat^{1,2}, Gaurav Pundir⁴, Harshda Saxena^{1,2}, Muhseen Musthafa⁵, Nihar Apte⁶, Sahil Saha⁷, and Sagar^{1,2}

¹Krittika - The Astronomy Club of IIT Bombay, Powai, Mumbai - 400076, India

²Indian Institute of Technology Bombay, Mumbai - 400076, India

³Indian institute of Technology Madras, Chennai, 600036, India

⁴Indian Institute of Science Education and Research Pune, Pune, 411008, India

⁵UM-DAE Centre for Excellence in Basic Sciences, Mumbai, 400098

⁶College of Engineering Pune, Pune, 411005, India

⁷Indian Institute of Science Education and Research Kolkata, Mohanpur, West Bengal, Kolkata, 741246, India

Copyright © 2021 Krittika IITB

PUBLISHED BY KRITTIKA: THE ASTRONOMY CLUB OF IIT BOMBAY

[GITHUB.COM/KRITTIKA/IITB](https://github.com/KRITTIKA/IITB)

First Release, September 2021

Abstract

The Asteroid Belt of our Solar system is a fascinating collection of objects located between Mars and Jupiter. It is hypothesized that these asteroids are remains of a planet that could have occupied the region between Mars and Jupiter. Another hypothesis suggests that the asteroid belt is the remains of planetesimals in that region that were too strongly perturbed by Jupiter's Gravity.

Whatever their origins may be, the Asteroid belt has evolved to have very peculiar characteristics, one of these is the presence of "Kirkwood Gaps".

First observed by Daniel Kirkwood in 1866, these are gaps or dips in the distribution of the semi-major axes of the orbits of the main-belt asteroids. The position of these gaps corresponds to the locations of Orbital Resonances with Jupiter.

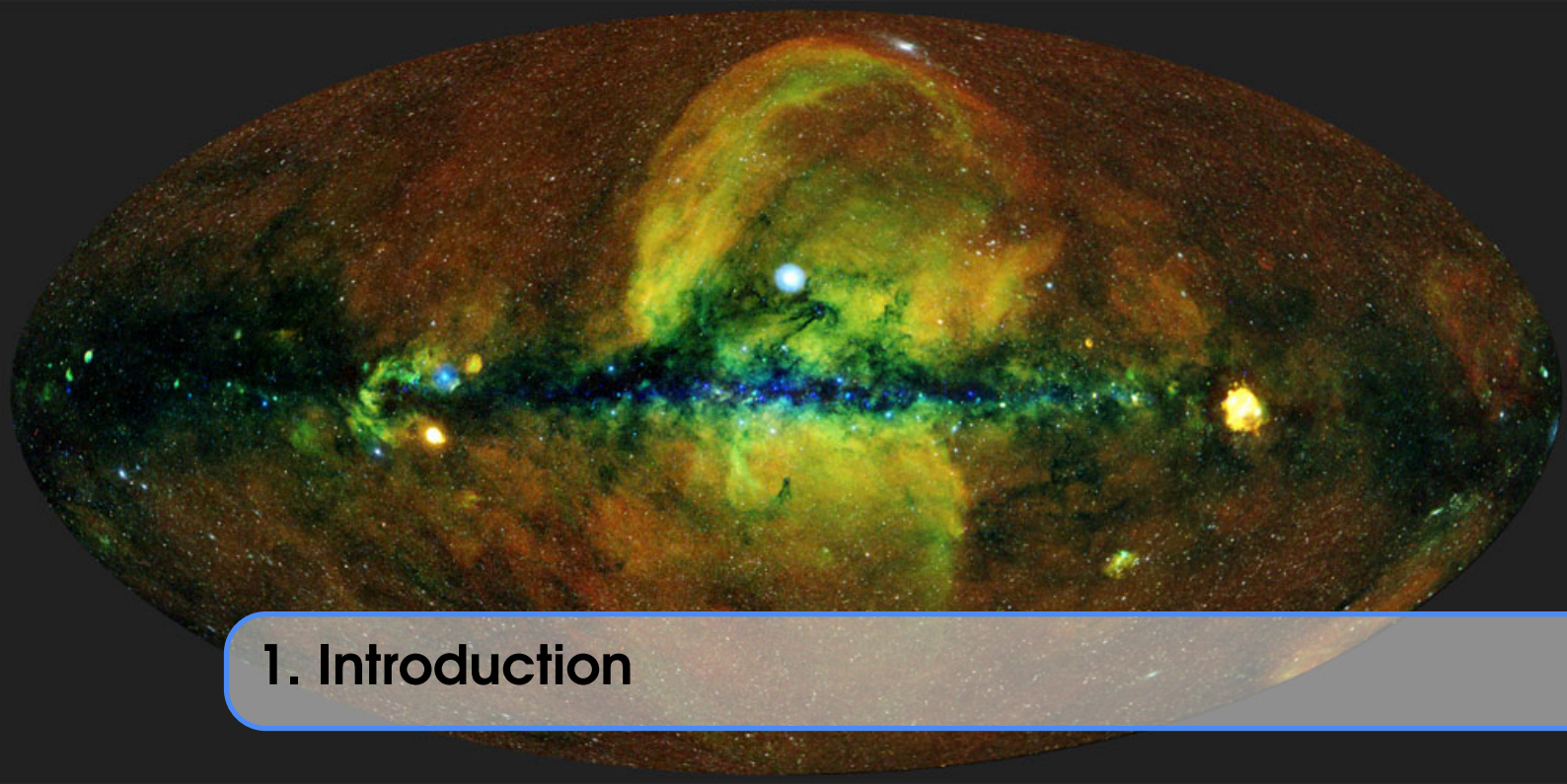
This Project aims at simulating the formation of the Kirkwood Gaps using numerical methods.



Contents

1	Introduction	5
1.0.1	Initial Discovery of The Asteroid Belt	5
1.0.2	The Kirkwood Gaps	6
2	Theory	8
2.0.1	The 2-Body Problem	8
2.0.2	The 3-Body Problem	9
2.0.3	The Restricted 3-Body Problem	9
3	Numerical Methods	11
3.1	The Integrator	11
4	Trajectories	14
4.0.1	Introduction	14
4.0.2	Tadpole Orbit	14
4.0.3	Horseshoe Orbit	15
4.0.4	Other Observed Trajectories	17
5	Simulations	18
5.1	Initial Distribution of Asteroids	18
5.2	Simulation of the Asteroid Belt	19
5.2.1	Simulation for 10,000 years	19
5.2.2	Simulation for 100,000 years	20
5.2.3	Simulation for 380,000 years	20
5.3	Discussion on why Gaps are not Visible in the Main Belt Simulations	22

6	Conclusion	23
6.1	Scope for More Precise Results and Further Applications	23
7	References	25
	References	25



1. Introduction

1.0.1 Initial Discovery of The Asteroid Belt

Johannes Kepler, best known for the famous Kepler's Laws of Planetary Motion, in 1596 predicted "between Mars and Jupiter, I place a planet".⁽¹⁾ Based on some of the empirical observations made at the time Kepler thought that there was too large of a gap between Mars and Jupiter.

Later in 1766, Johann Daniel Titius of Wittenberg⁽³⁾ noted "If one began a numerical sequence at 0, then included 3, 6, 12, 24, 48 . . . , doubling each time, and added 4 to each number and divided by 10, this produced a remarkably close approximation to the radii of the orbits of the known planets as measured in astronomical units provided one allowed for a "missing planet" (equivalent to 24 in the sequence) between the orbits of Mars and Jupiter". This came to be known as the Titius-Bode Law. In his footnote, Titius declared 'But should the Lord Architect have left that space empty? Not at all.'⁽⁴⁾

Their doubts were confirmed when in 1781 William Herschel⁽⁵⁾ found Uranus and the planet's orbit matched the empirical law almost perfectly, leading astronomers at the time to conclude that there has to be a planet between Mars and Jupiter. The culprit in play was the asteroid belt in between Mars and Jupiter. The asteroid belt is a torus-shaped region in the Solar System, located roughly between the orbits of the planets Jupiter and Mars. It contains many solid, irregularly shaped bodies, of many sizes called asteroids. The asteroid belt we are referring to (between Mars and Jupiter) is also called the Main Asteroid Belt or Main Belt to distinguish it from other asteroid populations in the Solar System such as near-Earth asteroids and Trojan asteroids.⁽⁴⁾

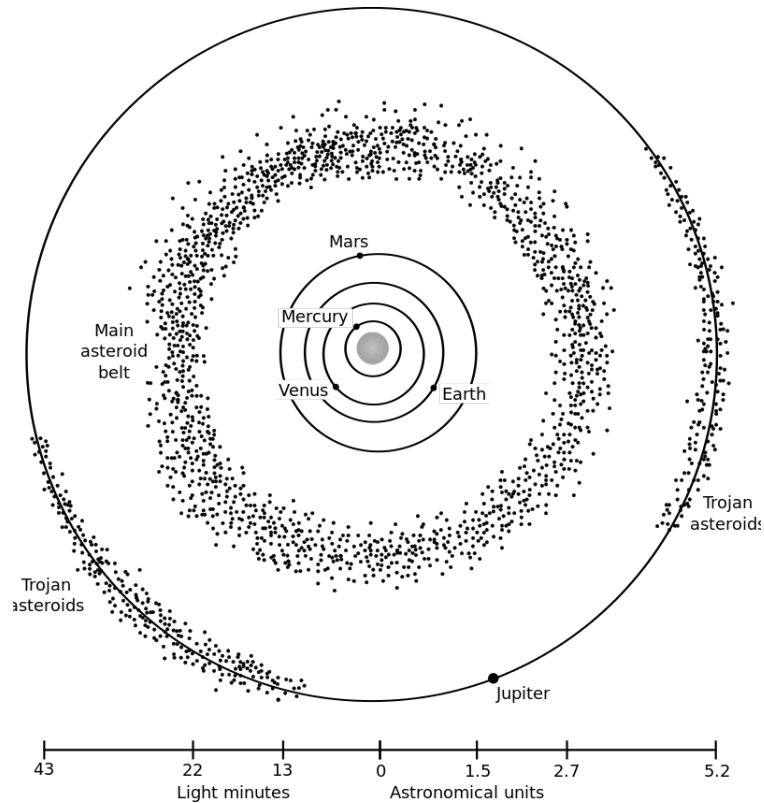


Figure 1: Asteroid Belts⁽⁶⁾

It is to be noted however, although the first known hints of the existence of asteroid belts came from the Titius-Bode Law, to date, there is no scientific reasoning for the law, and it also does not account for the orbital radius of Neptune, and it was probably just coincidental.

1.0.2 The Kirkwood Gaps

The distribution of asteroids in The Main Asteroid Belt is not uniform. There are regions of high asteroid density separated by gaps of low asteroid density⁽⁷⁾. Such gaps were first noticed by Kirkwood in 1866, who also correctly correlated their origin with the orbital resonances with Jupiter. Orbital resonances are defined as "Any system of two or more satellites (including planets) orbiting the same primary and whose orbital mean motions are in a ratio of small whole numbers"⁽⁸⁾. In such systems, when the bodies come close to one another they exert Gravitational Force on each other, changing each other's orbital velocity. In the Solar System, repeated orbital resonances cause the asteroids to fly out of the Solar System or to concentrate in certain regions of space. The gaps caused by this interaction are referred to as Kirkwood gaps⁽⁷⁾.

In this report, we attempt to numerically show that orbital resonances over a period of time indeed cause Kirkwood Gaps using Numerical Analysis.

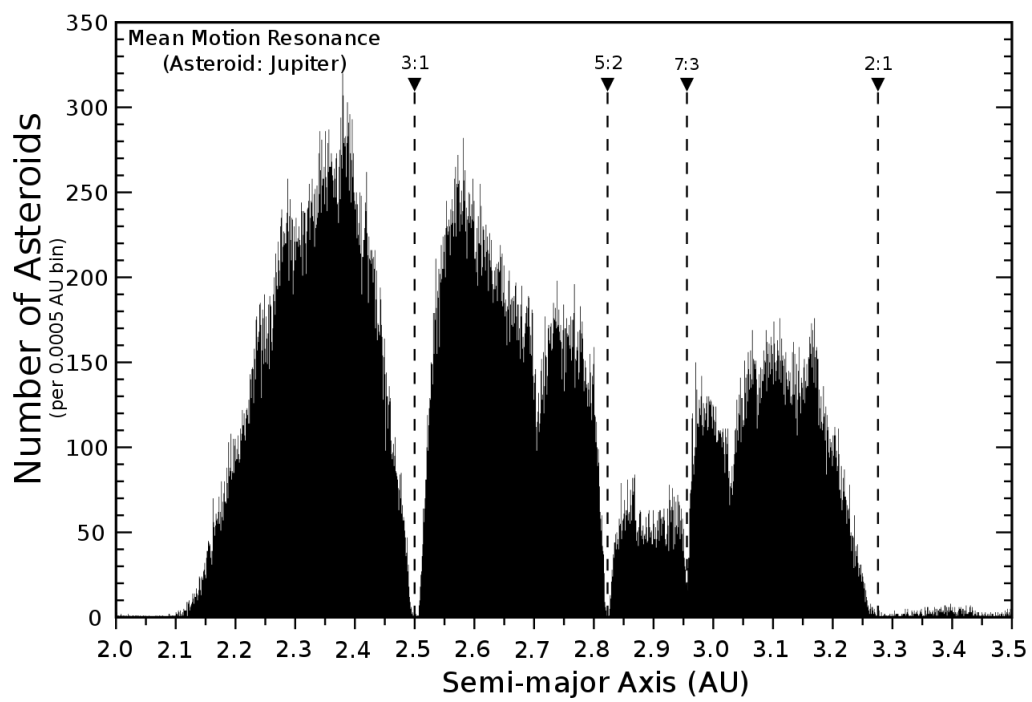


Figure 2: Kirkwood Gaps



2. Theory

2.0.1 The 2-Body Problem

Finding the future trajectories of two bodies given the force of interaction between them and their initial conditions constitutes the 2-body problem. We will only consider the gravitational case of the 2-body problem (also known as the Kepler problem). As per Newton's Law of Gravitation, the gravitational force between two point masses m_1 and m_2 , having position vectors \mathbf{r}_1 and \mathbf{r}_2 respectively, is given by -

$$\mathbf{F} = -\frac{Gm_1m_2}{|\mathbf{r}_1 - \mathbf{r}_2|^3}(\mathbf{r}_1 - \mathbf{r}_2) \quad (2.1)$$

Where G is the universal gravitational constant equal to $6.674 \times 10^{-11} \text{ Nm}^2/\text{kg}^2$. Combining this with Newton's second law of motion, we obtain the acceleration for the two bodies as -

$$\frac{d^2\mathbf{r}_1}{dt^2} = -\frac{Gm_2}{|\mathbf{r}_1 - \mathbf{r}_2|^3}(\mathbf{r}_1 - \mathbf{r}_2) \quad (2.2)$$

$$\frac{d^2\mathbf{r}_2}{dt^2} = -\frac{Gm_1}{|\mathbf{r}_1 - \mathbf{r}_2|^3}(\mathbf{r}_1 - \mathbf{r}_2) \quad (2.3)$$

A general solution to the Kepler problem exists and therefore, this problem is not chaotic. A very useful special case is when the two bodies are orbiting the combined centre of mass in circular motion. The common angular speed (ω) and the magnitude of total angular momentum of the system in such a case is given by -

$$\omega = \sqrt{\frac{G(m_1 + m_2)}{d^3}} \quad (2.4)$$

$$L = \mu\omega d^2 \quad (2.5)$$

Where d is the fixed distance between the two bodies and μ is the reduced mass, given by -

$$\mu = \frac{m_1 m_2}{m_1 + m_2}$$

A further simplification can be achieved by assuming the mass of one body to be negligible in comparison to the other ($m_2 \gg m_1$). In this case, m_2 can be assumed to remain stationary to a good approximation, and m_1 would execute circular motion around m_2 with angular speed (ω') given as -

$$\omega' = \sqrt{\frac{Gm_2}{d^3}} \quad (2.6)$$

This is also known as the angular Keplerian speed or the angular orbital speed of the smaller mass m_1 . Multiplying this with the distance d would give us the linear orbital speed.

2.0.2 The 3-Body Problem

The 3-body problem seeks solution to the trajectories of three bodies which are moving solely under the influence of each other's gravitational force, given their initial velocities and positions. Let m_1 , m_2 and m_3 be the three bodies and let their position vector at a general time be denoted by \mathbf{r}_1 , \mathbf{r}_2 and \mathbf{r}_3 . Their equations of motion are -

$$\frac{d^2 \mathbf{r}_1}{dt^2} = -\frac{Gm_2}{|\mathbf{r}_1 - \mathbf{r}_2|^3}(\mathbf{r}_1 - \mathbf{r}_2) - \frac{Gm_3}{|\mathbf{r}_1 - \mathbf{r}_3|^3}(\mathbf{r}_1 - \mathbf{r}_3) \quad (2.7)$$

$$\frac{d^2 \mathbf{r}_2}{dt^2} = -\frac{Gm_3}{|\mathbf{r}_2 - \mathbf{r}_3|^3}(\mathbf{r}_2 - \mathbf{r}_3) - \frac{Gm_1}{|\mathbf{r}_2 - \mathbf{r}_1|^3}(\mathbf{r}_2 - \mathbf{r}_1) \quad (2.8)$$

$$\frac{d^2 \mathbf{r}_3}{dt^2} = -\frac{Gm_1}{|\mathbf{r}_3 - \mathbf{r}_1|^3}(\mathbf{r}_3 - \mathbf{r}_1) - \frac{Gm_2}{|\mathbf{r}_3 - \mathbf{r}_2|^3}(\mathbf{r}_3 - \mathbf{r}_2) \quad (2.9)$$

The complexity of the 2-body problem increases drastically upon the addition of just one body, making the 3-body problem chaotic. No general analytical solution exists for the trajectories of the bodies in the 3-body problem, therefore we must seek numerical solutions.

2.0.3 The Restricted 3-Body Problem

Also known as the Reduced 3-body problem, the assumption that the mass of one of the three bodies is negligible as compared to the masses of the other two bodies is made here. We are then interested in the motion of this small body. Since our goal is to simulate an asteroid moving under the influence of Sun and Jupiter, it would be beneficial to make this assumption.

We will restrict the motion of the small body (the asteroid) to the plane of motion of the two bigger bodies (Sun and Jupiter). Since the eccentricity of Jupiter's orbit around the Sun is fairly low (≈ 0.049), we will assume its path to be circular. Moreover, it shall be convenient to work in a reference frame having origin at the centre of mass of Sun and Jupiter and rotating with the same angular velocity as the two bodies.

Let the coordinates of the asteroid be (x, y) in the rotating frame. We choose the x -axis to be such that the Sun and Jupiter always lie at $(x_s, 0)$ and $(x_j, 0)$ respectively

with $x_j > 0$. Let r_s and r_j be the distances of the asteroid to Sun and Jupiter, given by -

$$r_s = \sqrt{(x - x_s)^2 + y^2} \quad (2.10)$$

$$r_j = \sqrt{(x - x_j)^2 + y^2} \quad (2.11)$$

The equations of motion of the asteroid are then given by⁽²⁾ -

$$\frac{d^2x}{dt^2} - 2\frac{dy}{dt} = x - GM_s \frac{(x - x_s)}{r_s^3} - GM_j \frac{(x - x_j)}{r_j^3} \quad (2.12)$$

$$\frac{d^2y}{dt^2} + 2\frac{dx}{dt} = y - GM_s \frac{y}{r_s^3} - GM_j \frac{y}{r_j^3} \quad (2.13)$$

In this report, we adopt a system of units in which $M_s + M_j = 1$, the distance between the Sun and Jupiter $d = 1$, and the unit of time is such that the Gravitational constant, $G = 1$. Let the mass of Jupiter be μ and that of Sun be $1 - \mu$. We can also express x_s and x_j in terms of the masses as -

$$x_s = -\mu \quad (2.14)$$

$$x_j = 1 - \mu \quad (2.15)$$

The equations for the asteroid then become -

$$\frac{d^2x}{dt^2} - 2\frac{dy}{dt} = x - (1 - \mu) \frac{(x + \mu)}{r_s^3} - \mu \frac{(x - (1 - \mu))}{r_j^3} \quad (2.16)$$

$$\frac{d^2y}{dt^2} + 2\frac{dx}{dt} = y - (1 - \mu) \frac{y}{r_s^3} - \mu \frac{y}{r_j^3} \quad (2.17)$$

It should also be noted that in this system of units, 1 unit of time is equal to 1.89 years.



3. Numerical Methods

3.1 The Integrator

In order to calculate the trajectory following the derived equations in the restricted three body problem, we need to find a suitable algorithm. The methods commonly used include Runge-Kutta Fourth Order Method and Euler Method. However, we also attempted symplectic methods including Velocity Verlet Algorithm and Symplectic Euler Method. However, there are issues with all of these commonly used methods, especially concerning symplectic methods.

For the Euler Algorithm, it was not used as its accuracy is acceptable only over small time steps and a small time of calculation. We needed to simulate for 10,000 to 100,000 years for acceptable results and considered a 7-14 day time step which was not compatible.

For symplectic methods, the primary requirement is that the Hamiltonian of the system is preserved. In our case, the Hamiltonian has the expression :

$$H = T + V = \frac{1}{2}m(\dot{x}^2 + \dot{y}^2 + 2\omega x\dot{y} - 2\omega\dot{x}y) - \frac{1}{2}m\omega^2(x^2 + y^2) - \frac{GmM_1}{((x+r_1)^2 + y^2)^{\frac{1}{2}}} - \frac{GmM_2}{((x-r_2)^2 + y^2)^{\frac{1}{2}}}$$

From this, we notice that the acceleration obtained is velocity dependent, of the form :

$$\begin{aligned}\ddot{x} &= 2\dot{y} + x - \frac{\mu(x + \mu')}{((x + \mu')^2 + y^2)^{\frac{3}{2}}} - \frac{\mu'(x - \mu)}{((x - \mu)^2 + y^2)^{\frac{3}{2}}} \\ \ddot{y} &= -2\dot{x} + y - \frac{\mu y}{((x + \mu')^2 + y^2)^{\frac{3}{2}}} - \frac{\mu' y}{((x - \mu)^2 + y^2)^{\frac{3}{2}}}\end{aligned}$$

Thus, the Hamiltonian is not conserved and the actual conserved quantity in our case turns out to be (?) :

$$c = (\dot{x}^2 + \dot{y}^2 - x^2 - y^2) - \frac{\mu}{((x + \mu')^2 + y^2)} - \frac{\mu}{((x + \mu')^2 + y^2)}$$

And upon calculation we can see that the magnitude of energy rapidly increases with general symplectic methods thus rendering them unusable for any large span of time.

Coming to the implementation of Runge Kutta 4th order methods, we can see a high stability of the energy over a long span of time in the problem, providing accurate results, however in the range of 10,000 and above years with a 14 day time step, there is a small upward trend in the energy magnitude, thus it was not used.

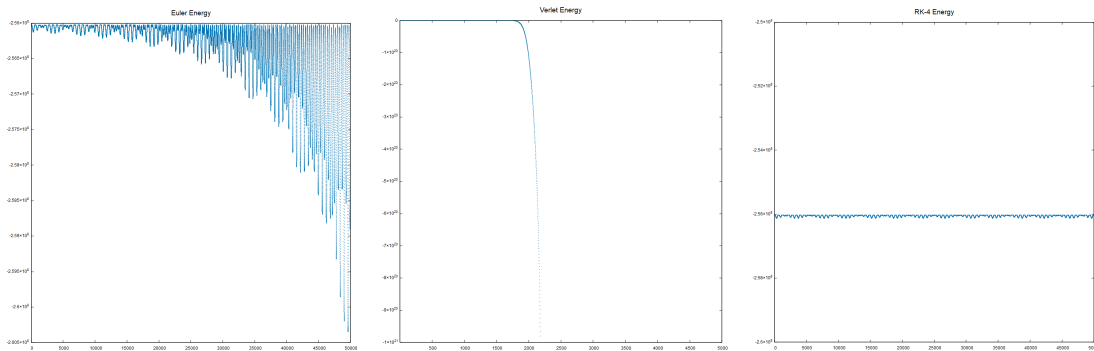


Figure 3: The above set of figures give us the comparison between three integrators, namely the Euler, the Verlet and the RK4 integrator. Even though RK4 looks very accurate, there are specific problems with RK4 which is explained in the paragraph above.

The final method of integration is a modification of the Euler method to include a midpoint, giving rise to the Euler-Richardson Algorithm. For the acceleration function $a = a(x, \dot{x})$, the method looks as follows:

$$a_n = a(x_n, \dot{x}_n)$$

$$\dot{x}_{mid} = \dot{x}_n + \frac{1}{2}a_n\Delta t$$

$$x_{mid} = x_n + \frac{1}{2}\dot{x}_n\Delta t$$

$$a_{mid} = a(x_{mid}, \dot{x}_{mid})$$

For the final value of the position and velocity :

$$\dot{x}_{n+1} = \dot{x}_n + a_{mid}\Delta t$$

$$x_{n+1} = x_n + v_{mid}\Delta t$$

For our calculations, this method of computing gave the most accurate results with deviation of maximum and minimum relative to the average being $\frac{\delta E}{E} = 4.14 \times 10^{-4}$.

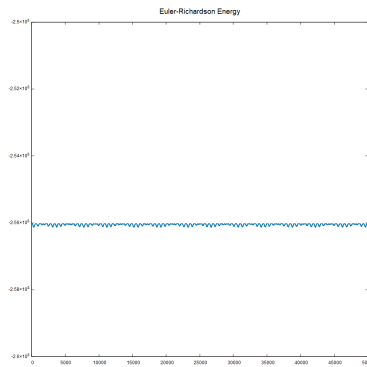


Figure 4: The above plot shows the deviations energy caused when we use the Euler-Richardson Algorithm are very small and this algorithm works best for our simulation.



4. Trajectories

4.0.1 Introduction

Here we present a few trajectories obtained by employing our integrator to just one asteroid. Typically the motion of an asteroid is chaotic and without any specific pattern (Figure 5), as one would expect. However, there are certain patterns observed when it is released near the Lagrange points.

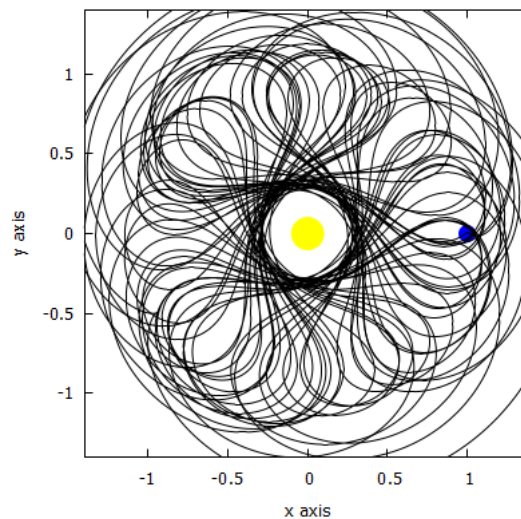
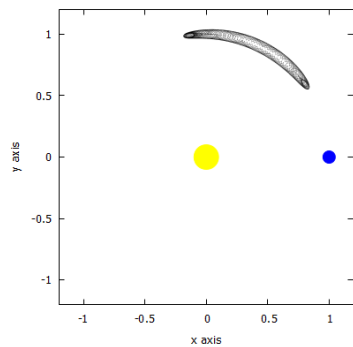


Figure 5: A chaotic trajectory

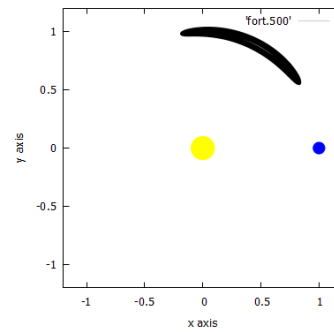
4.0.2 Tadpole Orbit

When placed at a very small distance from L4 and given zero initial velocity in the rotating frame, the asteroid executes a stable, periodic orbit which spreads

around L4 (Figure 6.a) . It retains its shape for at least 380,000 years (Figure 6.b).



(a) Trajectory for 1,900 years

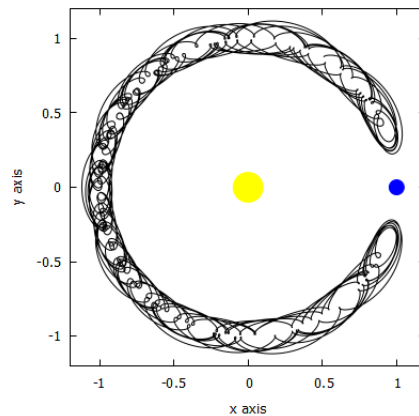


(b) Trajectory for 380,000 years

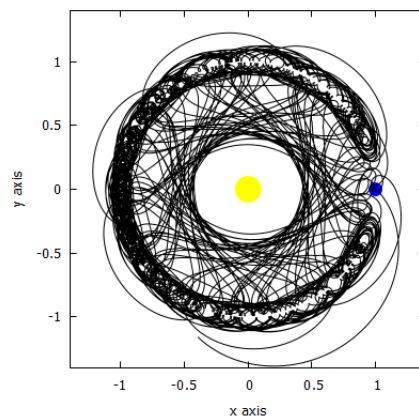
Figure 6

4.0.3 Horseshoe Orbit

Upon further slightly increasing its perturbation from L4, the trajectory develops into what is known as the 'horseshoe orbit' ⁽⁹⁾ (Figure 7.a). However, it soon becomes chaotic as shown in Figure 7.b.



(a) Trajectory for 1,900 years



(b) Trajectory for 7,000 years

Figure 7

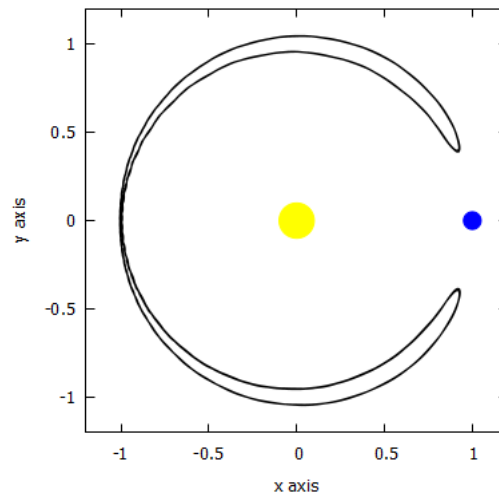
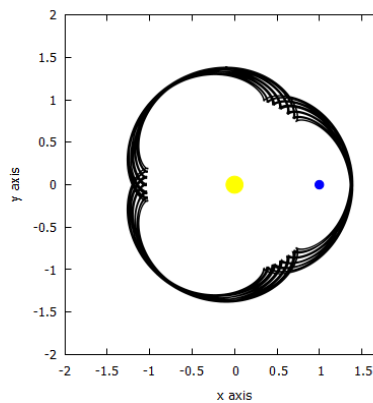


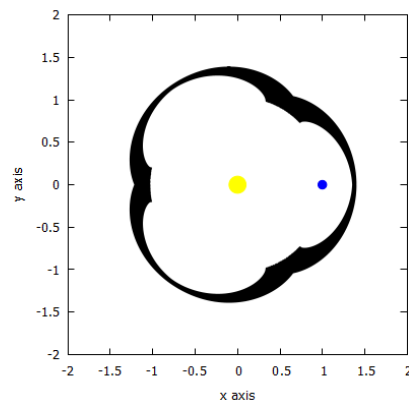
Figure 8: Horseshoe Orbit

A much neater horseshoe orbit is observed when the asteroid is released near L3 in Figure 8.

There are other interesting patterns as well, such as given in Figure 9.a obtained again by slightly displacing the asteroid near L4 in a different direction. This orbit is remarkably stable, with the asteroid remaining in it for at least 95,000 years as can be seen in Figure 9.b.



(a) Trajectory for 1,900 years



(b) Trajectory for 95,000 years

Figure 9

4.0.4 Other Observed Trajectories

Below we provide four plots for a third body placed near L1, L2 and L3. We can see that for all the cases, there is some restricted orbit for a short period of time but once the object gets close to either the Sun or Jupiter, it does not return. The placement on L3 results in another Horseshoe orbit like near L4 but without a spiral motion induced by the stable Lagrange points.

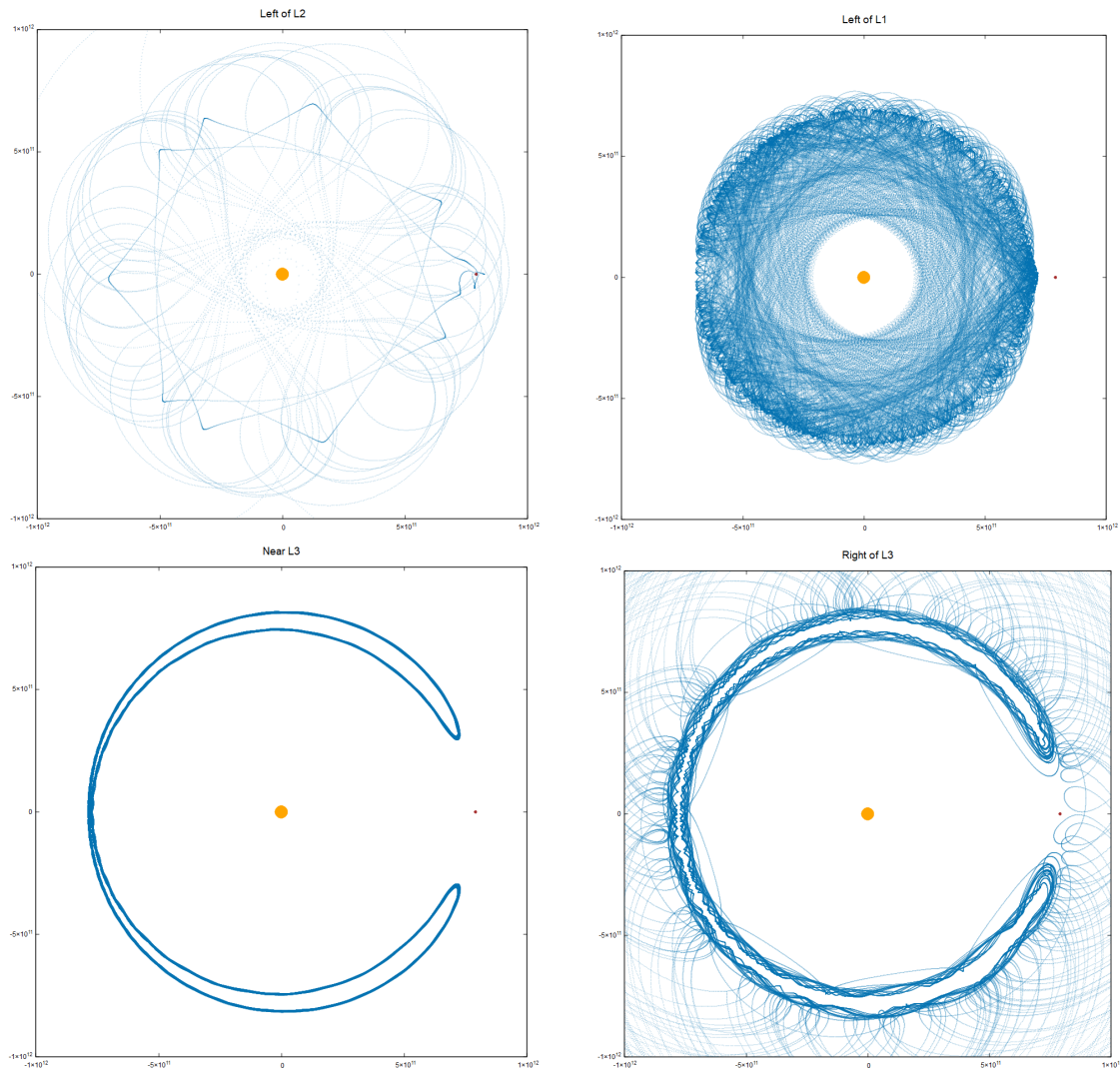


Figure 10: From Top Left, the trajectory for placement to the left of L2, Top Right, origin to the left of L1, Bottom Left, Horseshoe Orbit from near L3 and Bottom Right, unbounded trajectory with origin near L3.

5. Simulations

5.1 Initial Distribution of Asteroids

The main asteroid belt is placed in between Sun and Jupiter. In order to account for this in the simulation, 120,000 asteroids were considered to be uniformly distributed in radial range of 1×10^{11} to 10×10^{11} in all directions.

The rotation in circular orbits around sun was considered for each of them and initial velocities were provided according to the following equations:

$$\dot{x}_i = -y_i \left(\sqrt{\frac{GM_s}{x(i)^3}} - \omega \right), \dot{y}_i = x_i \left(\sqrt{\frac{GM_s}{x(i)^3}} - \omega \right)$$

We show the plot of the initial distribution below:

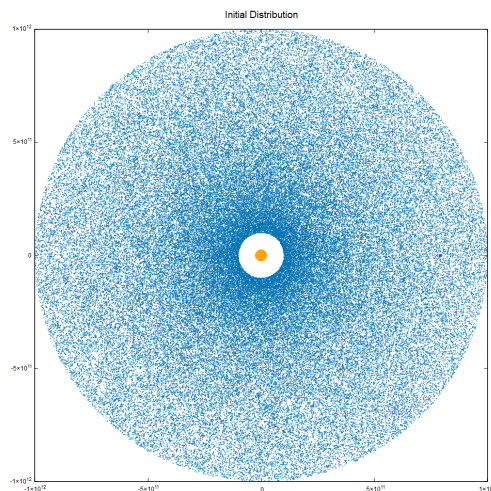


Figure 11: Initial Distribution of Asteroids

5.2 Simulation of the Asteroid Belt

The parameters used for the final simulation are listed below :

- Mass of Sun : $1.989 \times 10^{30} kg$
- Mass of Jupiter : $1.898 \times 10^{27} kg$
- Angular Velocity of Rotating Frame : $1.672 \times 10^{-8} rad/s$
- Gravitational Constant : $6.67 \times 10^{-11} units$
- Position of Sun : $(-743604142, 0)$
- Position of Jupiter : $(7.7926e11, 0)$

The initial conditions were set according to the values in the uniform distribution mentioned in Section 5.0.1 and similarly selected values of velocity.

We analyse the final results for different time gaps to obtain a better idea regarding the formation of the actual asteroid belt and gaps.

5.2.1 Simulation for 10,000 years

We first run our simulation at a 7 day time step for 520,000 counts thus obtaining around 10,000 years change of positions.

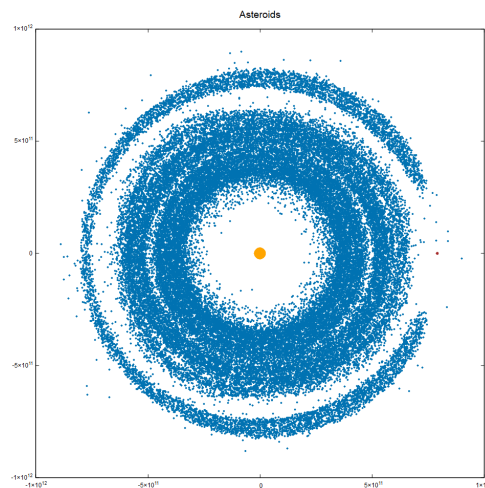


Figure 12.1 : Final Position of Asteroids after 10,000 years

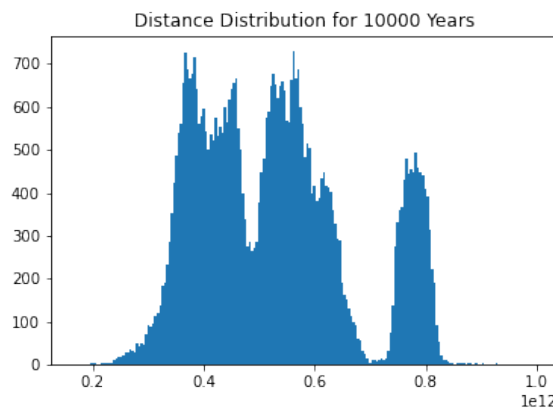


Figure 12.2 : Number of Asteroids against Distance from the Sun

From the figure we can see that there is an accumulation of a large number of asteroids near L4 and L5 lagrange points with a few transitioning along L3. There is

a formation of a clear inner belt with varying number of concentration of simulated points and an especially low concentration around the $4.75 \times 10^{11}m$ distance. The prominent gap in the neighbourhood of $7.5 \times 10^{11}m$ is the separation of the inner belt and the outer asteroids along the Jupiter orbit.

5.2.2 Simulation for 100,000 years

Now we move ahead to 100,000 years where stabilisation of the asteroid orbit starts. We obtain the following figures for a 7 day timestep and 5,200,000 counts thus going to nearly 100,000 years.

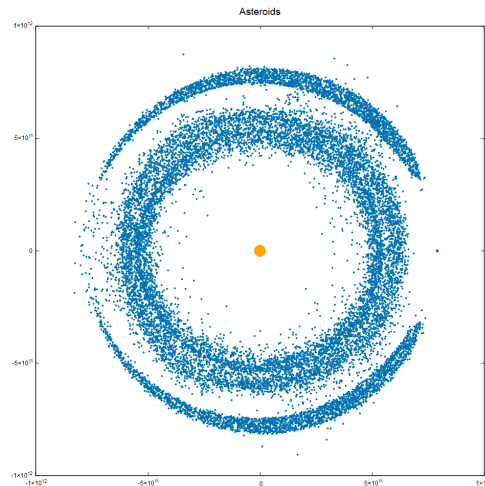


Figure 13.1 : Final Position of Asteroids after 100,000 years

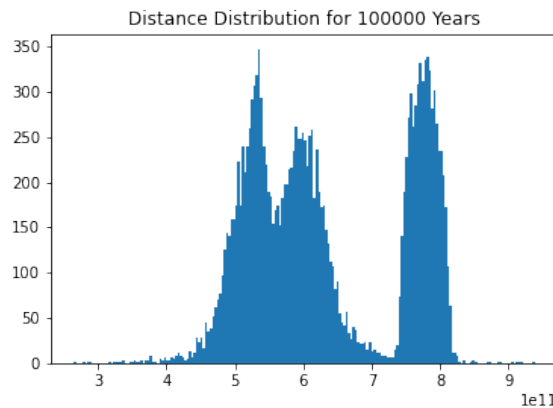


Figure 13.2 : Number of Asteroids against Distance from the Sun

Here we can also observe similar results with a prominent gap past $7e11$ m where the demarcation between the inner and outer belt is observed by extremely low number of asteroids. Near towards $5.5 \times 10^{11}m$ we observe the previously seen minima of number of asteroids and two consequent peaks on either side. The main belt seems to start at around $5 \times 10^{11}m$ and extends to $7 \times 10^{11}m$.

5.2.3 Simulation for 380,000 years

Approaching 380,000 years we can see that the asteroids are in stable orbits and follow an expected pattern. The time step is again 7 days and the count has been adjusted accordingly.

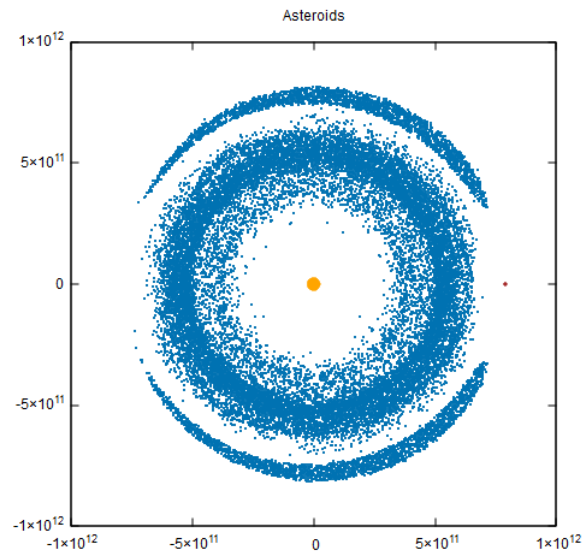


Figure 14.1 : Final Position of Asteroids after 100,000 years

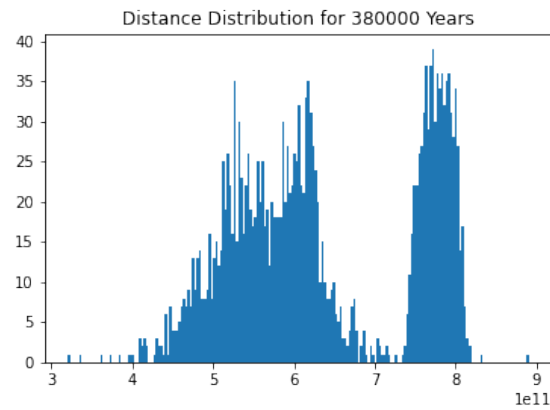


Figure 14.2 : Number of Asteroids against Distance from the Sun

However, we see no distinct minima in this case but there are periodic dips which follow the trend of the previous two figures. The main belt extends from $4 \times 10^{11}m$ to $7 \times 10^{11}m$ with the primary minima being near $5.5 \times 10^{11}m$.

5.3 Discussion on why Gaps are not Visible in the Main Belt Simulations

The reason that gaps in the distribution of semi major axes of the asteroids in the main asteroid belt is observed is due to Mean-Motion Resonance with the other planets, satellites etc. The resonance is best described by the fact that if an asteroid has a time period n and a larger mass orbiting around the sun has a time period m . If n and m are relatively small numbers like 1,2,3,..7, there are certain time intervals during which the two bodies line up and the larger mass pulls the asteroid away from its orbit slightly. This happens to all asteroids and thus "gaps" are formed in the main belt.

The primary reason these gaps are not visible during direct simulation is due to the eccentricity of the asteroid orbits themselves. Owing to the relatively uniform distribution over a certain range, the orbits often overlap and their tracks are covered by transitioning asteroids, covering up the gap(?).

However if we inspect the cases where simulation is done over relatively short time spans say 1,000 - 10,000 years, there are visible gaps as the orbits are not completely erratic in their eccentricities yet. Especially referring to Figure 10.2, the effect is extremely visible in the distribution of asteroids against distance from the sun with one clear minima and smaller relatively less obvious mean motion resonance induced gaps in the distribution.



6. Conclusion

The project initially started by testing out various integrators for numerically solving the differential equations related to basic orbital mechanics. After looking at the plots for deviations in energy, it was finally decided that the Euler-Richardson method worked best for this project. In parallel, knowledge about the governing equations for the reduced three body problem was also gathered from various sources.

Trajectories of the asteroids at various initial parameters was tested out which gave different results for different initial placements.

Finally, around 100,000 asteroids with varied initial parameters were generated and iterations were applied to each asteroid's parameters giving a final set of parameters after a considerable amount of time (thousands of years) which could be plotted. These plots resembled the Kirkwood gaps to a good accuracy given our approximations at the start.

6.1 Scope for More Precise Results and Further Applications

The results obtained can be refined with a few changes listed below :

- Considering the eccentricity of Jupiter Orbit into calculation
- More refined methods of integration can be used over larger spans like the Wisdom-Holman Algorithm
- To view the exact distribution of semi-major axes of fewer number of simulated asteroids over a larger span of time in millions of years
- Perturbation with more than one planet, including Saturn and Mars, which give more realistic results

The calculations of the restricted three body problem can be extended to map trajectories of close-passing asteroids to other planets, if distant systems are consid-

ered, there also arises the question of whether once out of orbit an asteroid can be caught by a different stellar or planetary system. The most direct application of these calculations would be to simulate the rings of Saturn perturbed by its moons and treat it similarly as we have treated the asteroid belt.



7. References

1. *Mysterium Cosmographicum*

https://en.wikipedia.org/wiki/Mysterium_Cosmographicum

2. Forest Ray Moulton. *An Introduction to Celestial Mechanics*. The Macmillan Company, New York, 1960.

3. Johann Daniel Titius, German astronomer and Professor

https://en.wikipedia.org/wiki/Johann_Daniel_Titius

4. <https://archive.ph/20120524184638/http://www-ssc.igpp.ucla.edu/dawn/background.html>

5. *Encyclopedia Britannica*

<https://www.britannica.com/biography/William-Herschel>

6. This is a public domain image. Credit : NASA

https://en.wikipedia.org/wiki/Asteroid#/media/File:Asteroid_Belt.svg

7. *SAO Encyclopedia of Astronomy*, Swinburne University

<https://astronomy.swin.edu.au/cosmos/k/Kirkwood+Gaps>

8. *Orbital resonance in the solar system*, Peale, S. J. (California, University, Santa Barbara, Calif.)

<https://ui.adsabs.harvard.edu/abs/1976ARA%26A..14..215P/abstract>

9. *Horseshoe orbit*, Wikipedia

https://en.wikipedia.org/wiki/Horseshoe_orbit

10. Maryam Tabeshian and Paul A. Wiegert 2016 *ApJ* 818 159

<https://iopscience.iop.org/article/10.3847/0004-637X/818/2/159>

11. *Hecuba-gap Asteroid*, Wikipedia

https://en.wikipedia.org/wiki/Hecuba-gap_asteroid1./main.tex